Force Field Influence on the Observation of π-Helical Protein Structures in Molecular Dynamics Simulations

Michael Feig,[†] Alexander D. MacKerell, Jr.,[‡] and Charles L. Brooks, III*[,†]

Department of Molecular Biology, TPC6, The Scripps Research Institute, 10550 North Torrey Pines Road, La Jolla, California 92037, and Department of Pharmaceutical Sciences, School of Pharmacy, University of Maryland, 20 North Pine Street, Baltimore, Maryland 21201

Received: October 23, 2002; In Final Form: January 10, 2003

In this study, we have investigated the sampling of π-helical conformations, with i, $i + 5$ hydrogen bonding, using empirical force fields. From replica exchange molecular dynamics simulations of the helical peptide acetyl-$(AAQAA)_3$-amide using the CHARMM22 force field and implicit solvent, we find rapid conversion from an initial α-helix to π-helical conformations. While this confirms similar studies of different peptides in explicit solvent, it does not agree with experimental data where π-helices are rarely observed. The sampling of π-helices is significantly diminished in favor of canonical α-helices when a newly extended CHARMM22/CMAP force field is used, where the backbone dihedral ϕ/ψ potential map in a vacuum is matched exactly to high-level quantum mechanical data for an alanine dipeptide model system. Energetic analysis shows that the difference between α- and π-helical conformations of the alanine dipeptide in a vacuum is 2.6 kcal/mol according to quantum mechanical calculations while both conformations are energetically equivalent in the unmodified CHARMM22 potential. Similar trends are also found in a number of other empirical force fields, suggesting that the observation of π-helical conformations in molecular dynamics simulations is mostly a force field artifact.

Introduction

The secondary structure of proteins is dominated by α-helices and β-sheets that are interconnected by turns and random coil loop sections to form a rich variety of tertiary fold topologies.[1] α-Helices and β-sheets are formed through distinct backbone conformations in the polypeptide chain that are commonly represented in Ramachandran plots through the backbone dihedral angles ϕ (C−N−C_α−C) and ψ (N−C_α−C−N).[2] ϕ/ψ values near (−60, −45) are typical for α-helices, while a more extended backbone with ϕ/ψ around (−90, 150) is necessary to form β-sheet structures. Both α- and β-regions are energetically preferred due to favorable atom packing. Further stability is gained from backbone hydrogen bonds that are formed between residues i and $i + 4$ along α-helices and across strands in β-sheets.[3]

Other, less frequently identified secondary structure motifs in protein structures include the more tightly wound 3_{10}-helix, the left-handed α_L-helix, and the wider π-helix with i, $i + 5$ hydrogen bonds (see Figure 1).[3,4] They correspond to less favorable areas in the Ramachandran plot and often require further stabilization through interactions within the protein or with ligands. In particular, the π-helix conformation[5,6] is rarely observed experimentally with its unfavorable energy attributed to cavity formation in the helix interior and entropic costs as compared to a regular α-helix.[5,7,8] In a very recent survey of PDB structures, 104 π-helix cases with an average helix length of 1.5 turns could be identified when liberal criteria were applied that allowed for bifurcated i, $i + 4$ and i, $i + 5$ hydrogen bonds.[9]

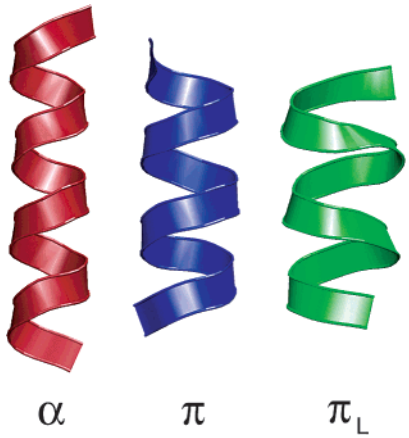

Figure 1. Backbone representation of a 15 residue peptide in α-helical (left), π-helical (center), and left-handed π-helical (right) conformations.

However, with a more stringent definition that required unambiguous i, $i + 5$ hydrogen bonds, only 10 occurrences were seen in another study.[8] In most of these cases, specific binding interactions have been implicated as stabilizing factors.[8] Another example of how a π-helical conformation may be stabilized was given recently in a designed peptide where two histidines, five residues apart, were aligned to form a zinc-binding site by forming a π-helix.[10] These experimental observations suggest that π-helical structures are only stable under exceptional circumstances.

In contrast, results from a number of recent molecular dynamics simulations have reported π-helical conformations in peptides of varying size and sequence. In simulations of the valine-rich surfactant protein C in water, the initial α-helix was transformed into a partial π-helix after ∼300 ps and persisted

* To whom correspondence should be addressed. Tel: (858)784-8035. Fax: (858)784-8688. E-mail: brooks@scripps.edu.
[†] The Scripps Research Institute.
[‡] University of Maryland.

10.1021/jp027293y CCC: $25.00
Published on Web 03/05/2003

until the end of the simulation (1 ns).[11] In peptides of the sequence $(AAXAA)_3$ that are experimentally found to form α-helices,[12−16] π-helical conformations occurred intermittently in molecular dynamics simulations, being observed in up to 23% of the total simulation time of some residues in $(AAQAA)_3$.[17] In simulations of the helical peptides alamethicin and melittin in methanol, π-helical hydrogen-bonding patterns are found near the center of the peptide chain, apparently contributing to an observed bending of the helix.[18,19] The transmembrane helical domain of the ErbB-2 receptor simulated in a lipid bilayer underwent reproducible transitions from α- to π-helix conformations in a series of nanosecond simulations.[20] Extensive simulations of the helical peptide $Y(MEARA)_6$ with an implicit solvation model revealed π-helix structures with a significant population between 5 and 40% during a 100 ns simulation.[21] Complete transitions from initial α-helices to π-helices were observed in simulations of three synthetic 13-residue peptides over the course of 5 ns simulations in aqueous solution with explicit water[22] and also in Ala_{10} and Aib_{10} peptides.[23] In a recent study of $A(AAAKA)_3$ with implicit solvent based on a generalized Born formalism[24] and using an efficient sampling protocol based on the Tsallis generalized potential,[25] π-helix conformations were observed along with canonical α- and 3_{10}-helices.[26] Toward the end of the same simulation, an interesting transition toward a left-handed π-helix structure was also observed (see Figure 1). Such a conformation has been indicated before from infrared spectra of poly(β-phenethyl L-aspartate),[27] but we are not aware of any examples in regular protein structures. Finally, in recent simulation studies that utilized the CHARMM22 force field, π-helical structures were observed in the peptides $Ac-A_{20}K + 2H^+$ and $Ac-V_{18}K + H^+$ near the C-terminal end of the peptides following proton addition near this site.[28,29]

The alanine dipeptide model compound is commonly used as a prototype for representing and optimizing backbone energetics in empirical force fields for all residues in peptides and proteins except glycine and proline. Figure 2 shows the vacuum potential energy surfaces for alanine dipeptide depending on ϕ and ψ values from the CHARMM22 force field[30] as well as high-level quantum mechanical (QM) calculations. It can be seen that the CHARMM22 energy function captures the general features of the QM energy surface but misses important features such as the more extended minimum around ϕ/ψ values of (70, 0) and the elevated region around (−75, −60), where π-helical conformations are found. We have recently extended the potential energy function of the CHARMM22 force field with ϕ/ψ cross-terms (in the sense of coupling ϕ/ψ angles through a map-based spline interpolation) in order to be able to accurately reproduce the QM ϕ/ψ map for the alanine dipeptide model.[31] When this extended potential, called CHARMM22/CMAP, was used for crystal simulations with explicit water, we found significantly better agreement with experimental data in terms of ϕ/ψ angle distributions and RMSD values suggesting that at least in this case a closer match to QM data leads to a more accurate empirical force field.[32]

In this paper, we will specifically address the sampling of π-helices when the extended CHARMM22/CMAP force field is used instead of the original CHARMM22 and put our results into perspective with respect to experimental data and previous simulations of π-helices.

Methods

As a model system, we have chosen the helical peptide Acetyl-$(AAQAA)_3$-amide which has been studied in detail by

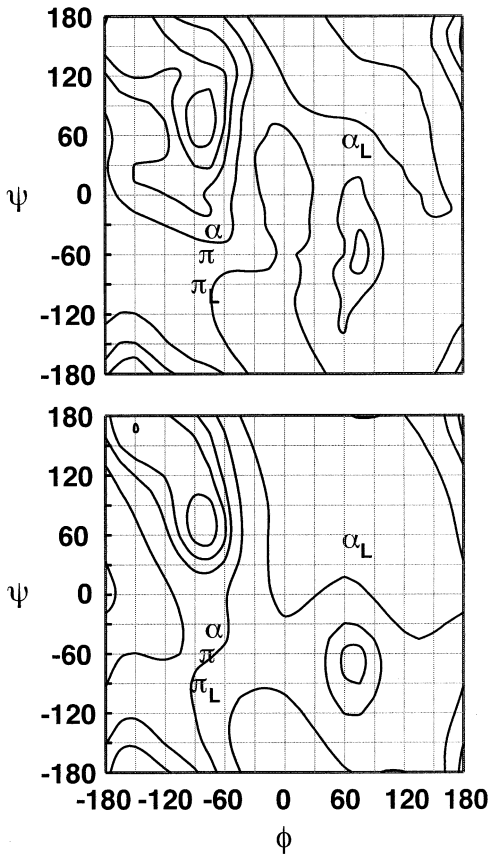

Figure 2. Alanine dipeptide potential maps in a vacuum for backbone dihedral angles ϕ (abscissa) and ψ (ordinate). Contour levels are shown at 1, 2, 3, 5, and 10 kcal/mol relative to the global minimum energy of the C7eq conformation around (−90, 75). A second minimum is present around (70, −70). The top map was calculated from ab initio calculations at the LMP2/cc-pVQZ(-g)//MP2/6-31G* level;[48,49] the bottom map represents the original CHARMM22 energy surface.

experiment[12] and was found to have the highest propensity for π-helix formation in simulations of similar model systems.[17]

We have carried out two replica exchange molecular dynamics simulations[33−35] of this peptide with implicit solvent. The first simulation was started from a regular α-helix structure using the original CHARMM22 force field.[30] In the second simulation, a π-helical starting conformation was used, obtained from the first simulation, in concert with the newly developed CHARMM22/CMAP force field with ϕ/ψ cross-term extensions.[31] As explained in more detail elsewhere,[31] the ϕ/ψ cross-terms were added through a grid-based map of energetic differences between the CHARMM22 and the QM surfaces for alanine dipeptide that is interpolated between grid points using cubic splines to obtain a smooth function for all ϕ/ψ values. This approach allows for reproduction of the QM alanine dipeptide energy surface with an overall RMS error of 0.04 kcal/mol. The reference QM surface was calculated at the LMP2/cc-pVTZ//MP2/6-31g* level. The accompanying CHARMM parameters, which were used here, are available upon request from the authors.

Replica exchange simulations,[33,36] where a number of simulation copies are run at different temperatures and are periodically exchanged according to Boltzmann criteria based on potential energy, were used to facilitate the crossing of barriers and greatly enhance sampling of conformational space. For the simulations described here, we used eight replicas with exponentially spaced temperatures from 250 to 450 K with exchange attempts at 1 ps intervals. For the implicit solvent description, we used a

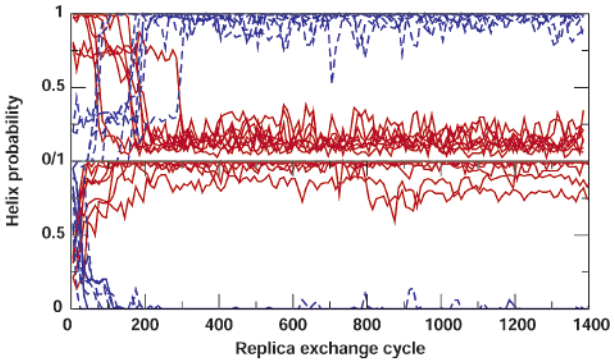

Figure 3. Evolution of α-helical (red, −) and π-helical (blue, - - -) conformations in replica exchange simulations of $(AAQAA)_3$ as measured by i, $i+4$ and i, $i+5$ hydrogen bonding, respectively. The fraction of hydrogen bonding among all possible hydrogen bonds (11 for an α-helix, 10 for a π-helix) is shown over the simulation time in picoseconds for each replica. The top graph shows simulation results with the original CHARMM22 force field with an α-helical starting conformation. The bottom graph shows results with CHARMM22/CMAP starting from a π-helix.

recently improved generalized born formalism.[37,38] Electrostatic cutoffs of 18 Å with a switching function beginning at 16 Å were used for nonbonded interactions during the simulation. The molecular dynamics simulations were carried out with the CHARMM program[39] in conjunction with the MMTSB Tool Set[40] where the replica exchange methodology is implemented.

Results

Two replica exchange simulations of acetyl-$(AAQAA)_3$-amide with the CHARMM22 and CHARMM22/CMAP force fields starting from α- and π-helical conformations, respectively, were carried out over 1.4 ns resulting in a combined simulation time of 11.2 ns for all eight replicas. To measure α-helix or π-helix formation for each replica, we have calculated the fraction of α-helical (i, $i+4$) and π-helical (i, $i+5$) hydrogen bonds between the backbone amide groups over the course of the simulations. For a 15-residue polypeptide, a maximum of 11 i, $i+4$ and 10 i, $i+5$ hydrogen bonds can be formed. As a definition of hydrogen bonding, we required the distance between the amine hydrogen and the carbonyl oxygen to be less than 3 Å as well as an N−H−O angle of more than 120°.

The resulting time series is shown in Figure 3. It can be seen that in the first simulation, with the regular CHARMM22 force field started from an α-helical conformation, all replicas undergo a complete transition to a π-helical structure within the first 300 ps of simulation time. For some replicas a mixed structure with partial π-helix content is formed immediately, and this conformation is maintained for up to 200 ps before the transition is completed. In other replicas, the entire helix is transformed cooperatively over the course of tens of picoseconds. In the second simulation, with the CHARMM22/CMAP force field, the model peptide very quickly adopts a regular α-helical conformation from the initial π-helix structure, losing all i, $i+5$ hydrogen bonds during the first 100 ps. During the course of this simulation, some replicas lose a fraction of i, $i+4$ hydrogen bonds. This does not occur at the expense of i, $i+5$ hydrogen bonds but because of thermal unfolding at higher temperatures where part of the helical structure is lost completely, in agreement with experiment.[12]

While a total simulation time of 1.4 ns for each replica may seem short, the enhanced sampling gained from the replica exchange scheme is expected to be equivalent to a much longer conventional single temperature molecular dynamics simulation at room temperature.[33] As an additional test, we also ran a longer replica exchange simulation of the same system, over 3.8 ns with the CHARMM22/CMAP force field, where the initial α-helical conformation was maintained throughout the simulation (data not shown). We have also observed the rapid transition from an α-helix to a π-helix in a single molecular dynamics run at room temperature after 7 ns during a total simulation of 12 ns when the CHARMM22 force field was used without the CMAP extension (data not shown). While a single simulation event is not statistically meaningful in any way, this time scale may be put into relation to the transition times of 100−300 ps seen in replica exchange simulations in order to illustrate the difference in sampling efficiency.

The effect of the force field on the sampling of π-helical conformations is further illustrated with ϕ/ψ potential energy maps of the alanine dipeptide, which include continuum solvent contributions from the generalized Born model in order to indicate which conformational regions are preferred in aqueous solution (see Figure 4). Comparing the QM/GBMV (top) map with the CHARMM22/GBMV map (center) reveals differences in the helical region around (−90, −30). The minimum in the QM-based map extends toward positive ψ values, and there is a rather steep increase in energy from the α-helical region toward more negative ψ values associated with a π-helix. The minimum in the CHARMM22 map, however, is centered around (−90, −60), encompassing π-helical conformations and extending into negative ψ values near −120° with an energy increase into the α-helical region. While these maps are for the alanine dipeptide and do not take into account all energetic contributions of helix formation such as interresidue nonbonded interactions, hydrogen bonding, and entropic costs, they reflect the inherent backbone energetics of both force fields. The data suggest a distinct bias toward π-helical backbone conformations in the CHARMM22 force field, which disappears when the underlying vacuum surface is matched to the corresponding QM surface as evidenced by the simulation data shown above.

In this context, it is also possible to address the occurrence of left-handed π-helical structures that have been reported recently[26] from simulations with CHARMM22 and a previous GB version.[24] For comparison, we have also calculated the alanine dipeptide surface with CHARMM22 and this older GB version. The resulting map, shown at the bottom of Figure 4, compares qualitatively with the surface based on the newer GB version (CHARMM22/GBMV, center) but with a single minimum region along $\phi = -90$ from π-helical conformations at $\psi = -60$ to extended conformations at $\psi = 150°$ while α-helical backbone conformations are even higher in energy. As Figure 4 shows, the dihedral angles found in a left-handed model π-helix lie all within or near the most favorable conformational regions of both CHARMM22 maps with best agreement when the older GB model is used, while in the QM-based map almost all of these ϕ/ψ values are in regions of higher energy.

Finally, we were interested whether these findings apply to other force fields, since π-helices were found in simulations with CHARMM19,[17,21] GROMOS,[11,41] and CVFF[18,19] in addition to simulations with CHARMM22.[22,23,26] In Table 1, the energy of the π-helical conformation (−75, 60) relative to the α-helical conformation (−60, −45) is presented for vacuum QM calculations at different levels of theory and for different force fields. It can be seen that all of the classical force fields in the table underestimate the energy penalty of 2.6 kcal/mol in going from α- to π-helical conformations as given from high-level

TABLE 1: Relative Potential Energy (in kcal/mol) between π-Helical and α-Helical Conformations of Alanine Dipeptide in Vacuum for Different Levels of Theory and Force Fields[a]

level of theory	$E(\pi) - E(\alpha)$	level of theory	$E(\pi) - E(\alpha)$
HF/6-31G*//HF/6-31G*	2.3	Amber 94	2.2
MP2/6-31G*//MP2/6-31G*	2.5	Amber 96	1.3
LMP2/cc-pVQZ//MP2/6-31G*	2.6	OPLS	1.2
CHARMM22/CMAP	2.6	GROMOS 96	−0.3
CHARMM22	0.0	GROMACS	0.1
CHARMM19	1.2		

[a] QM calculations were performed with Gaussian98[48] and Jaguar.[49] Classical force field energies were evaluated with the CHARMM program[39] with suitable parameter files[50] for the CHARMM,[30,39] Amber,[47] and OPLS[51] force fields. The energies for the GROMOS96[52] and GROMACS[53,54] force fields were evaluated with the GROMACS[53,54] program (Olle Edholm, personal communication). CHARMM22/CMAP denotes the CHARMM22 force field with a map-based dihedral cross-term as described in this paper. The alanine dipeptide structures were fully minimized with dihedral restraints before evaluating the energies.

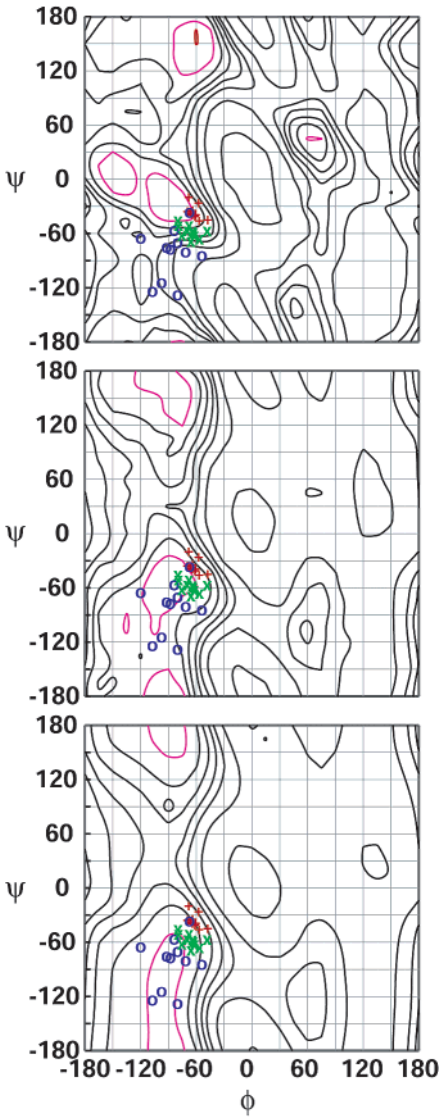

Figure 4. Alanine dipeptide potential maps with implicit solvation for ϕ and ψ as in Figure 2. The lowest energy contour line is shown in purple. Subsequent contour lines are at 1, 2, 3, 4, 6, and 11 kcal/mol. The top map (QM/GB) shows the combined energy of CHARMM22 with the CMAP correction,[31] which is pratically identical to the QM surface shown in Figure 2, and the GBMV generalized born implementation[37,38] for implicit solvation, the center map (CHARMM22/GBMV) shows the original CHARMM22 energy in combination with GBMV, and the original CHARMM22 energy in combination with an older generalized born implementation[24] is represented in the bottom map (CHARMM22/GB). For reference, ϕ/ψ dihedral angles from representative α-helical (red, +), π-helical (green, ×), and left-handed π-helical (blue, ○) structures obtained by simulation are indicated in all three maps.

QM calculations. While only Amber 94 provides a reasonable approximation, the energetic difference is reduced to 1.2−1.3 kcal/mol with CHARMM19, Amber 96, and OPLS. With CHARMM22, GROMOS96, and GROMACS, α- and π-helices are energetically equivalent in a vacuum, leading to a bias toward π-helices once contributions from solvation are added as shown above.

Discussion

From simulations of a helical model peptide, acetyl-$(AAQAA)_3$-amide, in solution, we find that if the CHARMM22 force field is used π-helical conformations with i, $i+5$ hydrogen bonds are preferred over regular α-helical structures with i, $i+4$ hydrogen bonding. While our simulations employed an implicit solvation scheme based on the generalized Born model, the results are in qualitative agreement with simulations of other peptides in explicit solvent.[22] However, the observation of π-helices in free peptides appears to be inconsistent with experimental data where π-helices are rarely found at all and usually require some form of additional stabilization. When the extended CHARMM22/CMAP force field is used, where ϕ/ψ cross-terms were added to accurately reproduce the QM surface of alanine dipeptide in a vacuum (Figure 2, top), the energetic balance shifts such that a regular α-helical structure becomes the most favorable conformation for the model peptide. Simultaneously, the π-helical conformations seen with the unmodified CHARMM22 force field are not sampled at all, in better agreement with experimental data. This would suggest that the CHARMM22 backbone potential based on the alanine dipeptide, in fact, provides a substantial bias toward sampling π-helical conformations.

Interestingly, π-helices that were found in experimental structures have average ϕ/ψ angles of $(-76, -41)$[9] as compared to $(-75, -60)$ in π-helices from simulations. The QM-based surface in Figure 4 shows that ϕ/ψ values around $(-76, -41)$ in solvated alanine dipeptide lie at the edge of the α-helical minimum while the energy increases significantly toward $(-75, -60)$. Therefore, the experimentally observed π-helical structures should still be accessible in simulations with the CHARMM22/CMAP force field if other energetic contributions are sufficiently favorable.

With regard to experimental evidence for π-helices, it should be stressed again that π-helical conformations, even around $(-76, -41)$, that lead to more than one $(i, i+5)$ consecutive hydrogen bond are found to be quite rare in recent surveys of PDB structures.[8,9,42] In the few cases where clear π-helices are observed, they appear to be stabilized by very specific, functionally relevant interactions[8] suggesting that π-helices, in general, are not favorable secondary structure elements of proteins.

Circular dichroism (CD) spectra of regular small peptides also do not suggest any significant fraction of π-helical conforma-

tions, although it has been suggested that α- and π-helical conformations may have indistinguishable CD spectra.[21] However, evidence for π-helicity was observed with CD in a Zn^{2+}-binding amphiphilic peptide that was specifically designed to form a π-helical structure.[10] Further experimental data are available from high-resolution ion mobility measurements of unsolvated and partially hydrated peptides.[28,29] In these studies, collision cross-sections were calculated for simulated peptide conformations and compared with measured values. It was found that for peptides where the simulated structures contained a significant fraction of π-helicity the calculated cross-sections significantly underestimated the experimental values while α-helical conformations were generally in good agreement with the measurements.[29] These data also suggest that significant populations of π-helical conformations as observed in some computer simulations are generally not supported by the available experimental evidence. The available data cannot exclude, however, that small populations of π-helices may be sampled at times.

It is not entirely clear to what extent QM energies in a vacuum provide the correct additive surface for simulations in aqueous solution, since alterations of the energetic properties of the peptide bond[43,44] and other possible solvent contributions are not taken into account. It is expected, however, that the true surface is approximated much better based on complete vacuum QM maps than with force field-based surfaces that have been fitted to vacuum QM energies of only a few selected conformations. The validity of this assumption has been confirmed with simulations presented here and elsewhere[31] that show improved sampling of dihedral conformations, in better agreement with experimental data, when the CHARMM22/CMAP surface is used. While we do see significant improvements if the vacuum QM surface is used directly, we found that further empirical corrections to that surface yield additional improvements that are being discussed elsewhere.[45]

Furthermore, it should be noted that the ϕ/ψ map in a peptide or protein environment will be influenced by the type of side chain,[46] which may not be fully represented through explicit interactions and may require modifications as compared to the alanine-based surface. This is certainly true for glycine and proline for which different surfaces are used in CHARMM22/CMAP, but further adjustments for other residues may be necessary in the future to obtain a more accurate sequence specific backbone representation.

We also find that the stability of π-helices vs α-helices is overestimated to a similar degree in most other commonly used force fields. This would suggest that the observation of π-helices with ϕ/ψ values around $(-75, -60)$ in simulations of peptides or proteins is force field-dependent and should be reevaluated carefully.

An explanation for why most force fields appear to overestimate the stability of π-helices is 2-fold: First, one should consider the difficulties of obtaining accurate QM reference energies for a large number of alanine dipeptide conformations at the time when most force fields were parametrized. Typically, only QM energies of selected relevant conformations were used to define the dihedral map with most of the attention focused on the well-known α- and β-conformations.[30,47]

Second, the combination of the usual one-dimensional cosine series dihedral terms for ϕ and ψ for representing the two-dimensional (ϕ,ψ) map limits the ability to reproduce a given map exactly even if a complete QM map would have been available as target data. In particular, it is difficult to express steep localized features of a two-dimensional function without using cross-terms. This applies especially to the steep increase in dihedral energy in order to match the QM surface from the α-helical region around $(-60, -45)$ to the adjacent π-helical region around $(-75, -60)$. Finally, we can make a similar argument for the observation of left-handed π-helices that appear to coincide particularly well with minima in the alanine dipeptide ϕ/ψ map with CHARMM22 and an older GB version, both of which were used in the simulations where these structures were seen.[26] In the QM-based map, all but one of the ϕ/ψ angles for the left-handed π-helix correspond to regions of higher energy in agreement with experimental data where such structures have not been found in regular proteins.

Conclusions

From simulations presented here and in the literature, it appears that most commonly used empirical force fields allow the sampling of π-helical conformations that are generally not observed experimentally. However, if the peptide backbone potential is corrected to reproduce a high-level QM surface for alanine dipeptide the π-helical region becomes significantly higher in energy so that only α-helical regions are sampled. This is in better agreement with experimental data. While we have applied this correction based on CHARMM22, we would expect similar benefits for other empirical force fields that show the same trend of overestimating the stability of π-helices.

Acknowledgment. We thank Olle Edholm for providing the alanine dipeptide energies with the Gromos and Gromacs force fields. Financial support from the NIH supported resource Multiscale Modeling Tools in Structural Biology (http://mmtsb.scripps.edu) (Grant RR12255 to CLB III), and NIH Grant GM51501 (to A.D.M., Jr.) is acknowledged.

References and Notes

(1) Richardson, J. S. *Adv. Protein Chem.* **1981**, *34*, 167.
(2) Ramachandran, G. N.; Ramakrishnan, C.; Sasisekharan, V. *J. Mol. Biol.* **1963**, *7*, 95.
(3) Baker, E. N.; Hubbard, R. E. *Prog. Biophys. Mol. Biol.* **1984**, *44*, 97.
(4) Barlow, D. J.; Thornton, J. M. *J. Mol. Biol.* **1988**, *201*, 601.
(5) Low, B. W.; Baybutt, R. B. *J. Am. Chem. Soc.* **1952**, *74*, 5806.
(6) Donohue, J. *Proc. Natl. Acad. Sci. U.S.A.* **1953**, *39*, 470.
(7) Rohl, C. A.; Doig, A. J. *Protein Sci.* **1996**, *5*, 1687.
(8) Weaver, T. M. *Protein Sci.* **1999**, *9*, 201.
(9) Fodje, M. N.; Al-Karadaghi, S. *Protein Eng.* **2002**, *15*, 353.
(10) Morgan, D. M.; Lynn, D. G. *Biochemistry* **2001**, *40*, 14020.
(11) Kovacs, H.; Mark, A. E.; Johansson, J.; van Gunsteren, W. F. *J. Mol. Biol.* **1995**, *247*, 808.
(12) Shalongo, W.; Dugad, L.; Stellwagen, E. *J. Am. Chem. Soc.* **1994**, *116*, 8288.
(13) Rohl, C. A.; Fiori, W.; Baldwin, R. L. *Proc. Natl. Acad. Sci. U.S.A.* **1999**, *96*, 3682.
(14) Williams, L.; Kather, K.; Kemp, D. S. *J. Am. Chem. Soc.* **1998**, *1998*, 11033.
(15) Lacroix, E.; Viguera, A. R.; Serrano, L. *J. Mol. Biol.* **1998**, *284*, 173.
(16) Padmanabhan, S.; York, E. J.; Stewart, J. M.; Baldwin, R. L. *J. Mol. Biol.* **1996**, *257*, 726.
(17) Shirley, W. A.; Brooks, C. L., III. *Proteins* **1997**, *28*, 59.
(18) Gibbs, N.; Sessions, R. B.; Williams, P. B.; Dempsey, C. E. *Biophys. J.* **1997**, *72*, 2490.
(19) Sessions, R. B.; Gibbs, N.; Dempsey, C. E. *Biophys. J.* **1998**, *74*, 138.
(20) Duneau, J.-P.; Crouzy, S.; Chapron, Y.; Genest, M. *Theor. Chem. Acc.* **1999**, *101*, 87.
(21) Hiltpold, A.; Ferrara, P.; Gsponer, J.; Caflish, A. *J. Phys. Chem. B* **2000**, *104*, 10080.
(22) Lee, K.-H.; Benson, D. R.; Kuczera, K. *Biochemistry* **2000**, *39*, 13737.
(23) Mahadevan, J.; Lee, K.-H.; Kuczera, K. *J. Phys. Chem. B* **2001**, *105*, 1863.

(24) Dominy, B. N.; Brooks, C. L., III. *J. Phys. Chem. B* **1999**, *103*, 3765.
(25) Pak, Y.; Wang, S. *J. Chem. Phys.* **1999**, *111*, 4359.
(26) Pak, Y.; Jang, S.; Shin, S. *J. Chem. Phys.* **2002**, *116*, 6831.
(27) Sasaki, S.; Yasumoto, Y.; Uematsu, I. *Macromolecules* **1981**, *14*, 1797.
(28) Kinnear, B. S.; Kaleta, D. T.; Kohtani, M.; Hudgins, R. R.; Jarrold, M. F. *J. Am. Chem. Soc.* **2000**, *122*, 9243.
(29) Kohtani, M.; Jarrold, M. F. *J. Am. Chem. Soc.* **2002**, *124*, 11148.
(30) MacKerell, A. D.; Bashford, D.; Bellott, M.; Dunbrack, J. D.; Evanseck, M. J.; Field, M. J.; Fischer, S.; Gao, J.; Guo, H.; Ha, S.; Joseph-McCarthy, D.; Kuchnir, L.; Kuczera, K.; Lau, F. T. K.; Mattos, C.; Michnick, S.; Ngo, T.; Nguyen, D. T.; Prodhom, B.; Reiher, W. E.; Roux, B.; Schlenkrich, M.; Smith, J. C.; Stote, R.; Straub, J.; Watanabe, M.; Wiorkiewicz-Kuczera, J.; Yin, D.; Karplus, M. *J. Phys. Chem. B* **1998**, *102*, 3586.
(31) MacKerell, A. D., Jr.; Feig, M.; Brooks, C. L., III. Manuscript in preparation.
(32) Beachy, M. D.; Chasman, D.; Murphy, R. B.; Halgren, T. A.; Friesner, R. A. *J. Am. Chem. Soc.* **1997**, *119*, 5908.
(33) Sugita, Y.; Okamoto, Y. *Chem. Phys. Lett.* **1999**, *314*, 141.
(34) Zhou, R.; Berne, B. J.; Germain, R. *Proc. Natl. Acad. Sci. U.S.A.* **2001**, *98*, 14931.
(35) Garcia, A. E.; Sanbonmatsu, K. Y. *Proc. Natl. Acad. Sci. U.S.A.* **2002**, *99*, 2782.
(36) Hansmann, U. H. E. *Chem. Phys. Lett.* **1997**, *281*, 140.
(37) Lee, M. S.; Salsbury, F. R., Jr.; Brooks, C. L., III. *J. Chem. Phys*. **2002**, *116*, 10606.
(38) Lee, M. S.; Feig, M.; Salsbury, F. R., Jr.; Brooks, C. L., III. *J. Chem. Phys.*, in press.
(39) Brooks, B. R.; Bruccoleri, R. E.; Olafson, B. D.; States, D. J.; Swaminathan, S.; Karplus, M. *J. Comput. Chem.* **1983**, *4*, 187.
(40) Feig, M.; Karanicolas, J.; Brooks, C. L., III. *MMTSB NIH Research Resource*; The Scripps Research Institute: La Jolla, CA, 2001.
(41) Sajot, N.; Garnier, N.; Genest, M. *Theor. Chem. Acc.* **1999**, *101*, 67.
(42) Rajashankar, K. R.; Ramakumar, S. *Protein Sci.* **1996**, *5*, 932.
(43) Guo, H.; Karplus, M. *J. Phys. Chem.* **1994**, *98*, 7104.
(44) Guo, H.; Karplus, M. *J. Phys. Chem.* **1992**, *96*, 7273.
(45) MacKerell, A. D., Jr.; Feig, M.; Brooks, C. L., III. Manuscript in preparation.
(46) Dunbrack, J.; Roland, L.; Karplus, M. *Nat. Struct. Biol.* **1994**, *1*, 334.
(47) Cornell, W. D.; Cieplak, P.; Bayly, C. I.; Gould, I. R.; Merz, K. M.; Ferguson, D. M.; Spellmeyer, D. C.; Fox, T.; Caldwell, J. W.; Kollman, P. A. *J. Am. Chem. Soc.* **1995**, *117*, 5179.
(48) Frisch, M. J.; Trucks, G. W.; Schlegel, H. B.; Scuseria, G. E.; Robb, M. A.; Cheeseman, J. R.; Zakrzewski, V. G.; Montgomery, J. A., Jr.; Stratmann, R. E.; Burant, J. C.; Dapprich, S.; Millam, J. M.; Daniels, A. D.; Kudin, K. N.; Strain, M. C.; Farkas, O.; Tomasi, J.; Barone, V.; Cossi, M.; Cammi, R.; Mennucci, B.; Pomelli, C.; Adamo, C.; Clifford, S.; Ochterski, J.; Petersson, G. A.; Ayala, P. Y.; Cui, Q.; Morokuma, K.; Malick, D. K.; Rabuck, A. D.; Raghavachari, K.; Foresman, J. B.; Cioslowski, J.; Ortiz, J. V.; Stefanov, B. B.; Liu, G.; Liashenko, A.; Piskorz, P.; Komaromi, I.; Gomperts, R.; Martin, R. L.; Fox, D. J.; Keith, T.; Al-Laham, M. A.; Peng, C. Y.; Nanayakkara, A.; Gonzalez, C.; Challacombe, M.; Gill, P. M. W.; Johnson, B. G.; Chen, W.; Wong, M. W.; Andres, J. L.; Head-Gordon, M.; Replogle, E. S.; Pople, J. A. *Gaussian 98*; Gaussian, Inc.: Pittsburgh, PA, 1998.
(49) Schrödinger, Inc. Jaguar, 2000.
(50) Price, D. J.; Brooks, C. L., III. *J. Comput. Chem.* **2002**, *23*, 1045.
(51) Jorgensen, W. L.; Maxwell, D. S.; Tirado-Rives, J. *J. Am. Chem. Soc.* **1996**, *118*, 11225.
(52) van Gunsteren, W. F.; Billeter, S. R.; Eising, A. A.; Huenenberger, P. H.; Krueger, P.; Mark, A. E.; Scott, W. R. P.; Tirono, I. G. *Vdf Hochschulverlage AG an der ETH Zürich* **1996**.
(53) Berendsen, H. J. C.; van der Spoel, D.; van Drunen, R. *Comput. Phys. Commun.* **1995**, *91*, 43.
(54) Lindahl, E.; Hess, B.; van der Spoel, D. *J. Mol. Model.* **2001**, *7*, 306.